CURVELET FUSION OF MR AND CT IMAGES

**F. E. Ali, I. M. El-Dokany, A. A. Saad
and F. E. Abd El-Samie**

Department of Electronics and Electrical Communications
Faculty of Electronic Engineering
Menoufia University
32952, Menouf, Egypt

Abstract—This paper presents a curvelet based approach for the fusion of magnetic resonance (MR) and computed tomography (CT) images. The objective of the fusion of an MR image and a CT image of the same organ is to obtain a single image containing as much information as possible about that organ for diagnosis. Some attempts have been proposed for the fusion of MR and CT images using the wavelet transform. Since medical images have several objects and curved shapes, it is expected that the curvelet transform would be better in their fusion. The simulation results show the superiority of the curvelet transform to the wavelet transform in the fusion of MR and CT images from both the visual quality and the peak signal to noise ratio (PSNR) points of view.

1. INTRODUCTION

Image fusion is the process of merging two images of the same scene to form a single image with as much information as possible. Image fusion is important in many different image processing fields such as satellite imaging, remote sensing and medical imaging. The study in the field of image fusion has evolved to serve the advance in satellite imaging and then, it has been extended to the field of medical imaging. Several fusion algorithms have been proposed extending from the simple averaging to the curvelet transform. Algorithms such as the intensity, hue and saturation (IHS) algorithm and the wavelet fusion algorithm have proved to be successful in satellite image fusion. The IHS algorithm belongs to the family of color image fusion algorithms [1–3]. The wavelet fusion algorithm has also succeeded in both satellite and medical image fusion applications [3–5]. The basic limitation of

the wavelet fusion algorithm is in the fusion of curved shapes. Thus, there is a need for another algorithm that can handle curved shapes efficiently. So, the application of the curvelet transform for curved object image fusion would result in a better fusion efficiency. A few attempts of curvelet fusion have been made in the fusion of satellite images but no attempts have been made in the fusion of medical images [1, 2, 6].

The main objective of medical imaging is to obtain a high resolution image with as much details as possible for the sake of diagnosis. There are several medical imaging techniques such as the MR and the CT techniques. Both techniques give special sophisticated characteristics of the organ to be imaged. So, it is expected that the fusion of the MR and the CT images of the same organ would result in an integrated image of much more details. Researchers have made few attempts for the fusion of the MR and the CT images [4, 5, 7]. Most of these attempts are directed towards the application of the wavelet transform for this purpose. Due to the limited ability of the wavelet transform to deal with images having curved shapes, the application of the curvelet transform for MR and CT image fusion is presented in this paper.

The curvelet transform is based on the segmentation of the whole image into small overlapping tiles and then, the ridgelet transform is applied to each tile. The purpose of the segmentation process is to approximate curved lines by small straight lines. The overlapping of tiles aims at avoiding edge effects. The ridgelet transform itself is a 1-D wavelet transform applied on the Radon transform of each tile, which is a tool of shape detection. The curvelet transform was firstly proposed for image denoising [8–10]. Some researchers tried to apply it in satellite image fusion [1, 2, 6]. Because of its ability to deal with curved shapes, the application of the curvelet transform in medical image fusion would result in better fusion results than that obtained using the wavelet transform.

The rest of the paper is organized as follows. Section 2 reviews the wavelet fusion algorithm. Section 3 presents the mathematical basis of the curvelet transform. Section 4 presents the proposed curvelet fusion algorithm for MR and CT images. Section 5 gives the experimental results. Finally, section 6 gives the concluding remarks.

2. WAVELET FUSION

The most common form of transform type image fusion algorithms is the wavelet fusion algorithm due to its simplicity and its ability to preserve the time and frequency details of the images to be fused [11].
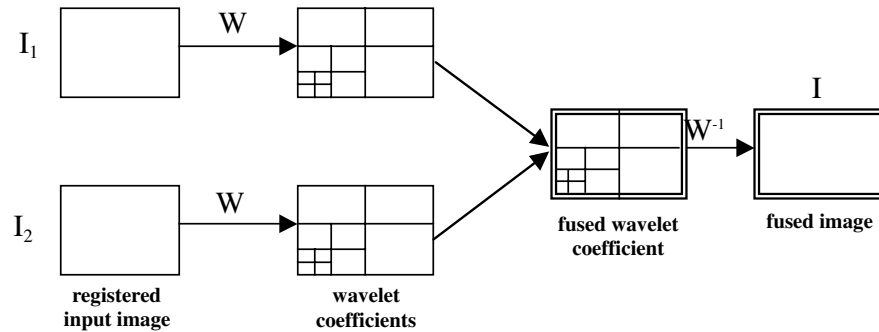
Figure 1. Wavelet fusion of two images.

A schematic diagram of the wavelet fusion algorithm of two registered images $I_1(x_1, x_2)$ and $I_2(x_1, x_2)$ is depicted in Fig. 1. It can be represented by the following equation:

$$I(x_1, x_2) = W^{-1}(\phi(W(I_1(x_1, x_2)), W(I_2(x_1, x_2)))). \qquad (1)$$

where W, W^{-1} and ϕ are the wavelet transform operator, the inverse wavelet transform operator and the fusion rule, respectively. There are several wavelet fusion rules, that can be used for the selection of the wavelet coefficients from the wavelet transforms of the images to be fused. The most frequently used rule is the maximum frequency rule which selects the coefficients that have the maximum absolute values [4, 5, 11].

The wavelet transform concentrates on representing the image in multiscales and it's appropriate to represent linear edges. For curved edges, the accuracy of edge localization in the wavelet transform is low. So, there is a need for an alternative approach which has a high accuracy of curve localization such as the curvelet transform.

3. THE CURVELET TRANSFORM

The curvelet transform has evolved as a tool for the representation of curved shapes in graphical applications. Then, it was extended to the fields of edge detection and image denoising [9, 10]. Recently, some authors have proposed the application of the curvelet transform in image fusion [1, 2].

The algorithm of the curvelet transform of an image P can be summarized in the following steps [8–10]:

 A) The image P is split up into three subbands Δ_1, Δ_2 and P_3 using the additive wavelet transform

B) Tiling is performed on the subbands Δ_1 and Δ_2.

C) The discrete ridgelet transform is performed on each tile of the subbands Δ_1 and Δ_2.

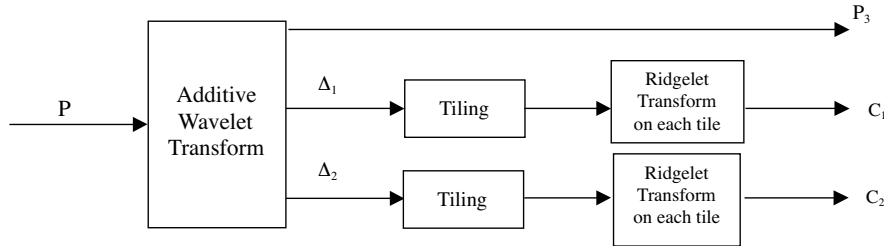A schematic diagram of the curvelet transform is depicted in Fig. 2.

Figure 2. Discrete curvelet transform of an image P.

A detailed description of these steps is presented below.

3.1. Subband Filtering

The purpose of this step is to decompose the image into additive components; each of which is a subband of that image. This step isolates the different frequency components of the image into different planes without down sampling as in the traditional wavelet transform. The "*a trous*" algorithm given below is used for this purpose [2, 3].

Given an image P, it is possible to construct the sequence of approximations:

$$f_1(P) = P_1, \quad f_2(P_1) = P_2, \quad f_3(P_2) = P_3, \ldots f_n(P_{n-1}) = P_n \quad (2)$$

where n is an integer which is preferred to be equal to 3. To construct this sequence, successive convolutions with a certain lowpass kernel are performed. The functions f_1, f_2, f_3, and f_n mean convolutions with this kernel which is given by [3]:

$$H = \frac{1}{256} \begin{pmatrix} 1 & 4 & 6 & 4 & 1 \\ 4 & 16 & 24 & 16 & 4 \\ 6 & 24 & 36 & 24 & 6 \\ 4 & 16 & 24 & 16 & 4 \\ 1 & 4 & 6 & 4 & 1 \end{pmatrix} \quad (3)$$

The wavelet planes are computed as the differences between two consecutive approximations P_{l-1} and P_l, i.e.,

$$\Delta_l = P_{l-1} - P_l \quad (4)$$

Thus, the curvelet reconstruction formula is given by:

$$P = \sum_{l=1}^{n-1} \Delta_l + P_n \tag{5}$$

3.2. Tiling

Tiling is the process by which the image is divided into overlapping tiles. These tiles are small in dimensions to transform curved lines into small straight lines in the subbands Δ_1 and Δ_2 [11–13]. The tiling improves the ability of the curvelet transform to handle curved edges.

3.3. Ridgelet Transform

The ridgelet transform belongs to the family of discrete transforms employing basis functions. To facilitate its mathematical representation, it can be viewed as a wavelet analysis in the Radon domain. The Radon transform itself is a tool of shape detection. So, the ridgelet transform is primarily a tool of ridge detection or shape detection of the objects in an image.

The ridgelet basis function is given by [1, 2, 9, 10]:

$$\psi_{a,b,\theta}(x_1, x_2) = a^{-1/2} \psi \left(\frac{(x_1 \cos \theta + x_2 \sin \theta - b)}{a} \right) \tag{6}$$

for each $a > 0$, each $b \in \mathbf{R}$ and each $\theta \in [0, 2\pi)$. This function is constant along lines $x_1 \cos \theta + x_2 \sin \theta = const.$

Thus, the ridgelet coefficients of an image $f(x_1, x_2)$ are represented by:

$$R_f(a, b, \theta) = \int_{-\infty}^{\infty} \int_{-\infty}^{\infty} \psi_{a,b,\theta}(x_1, x_2) f(x_1, x_2) dx_1 dx_2 \tag{7}$$

This transform is invertible and the reconstruction formula is given by:

$$f(x_1, x_2) = \int_{0}^{2\pi} \int_{-\infty}^{\infty} \int_{0}^{\infty} R_f(a, b, \theta) \psi_{a,b,\theta}(x_1, x_2) \frac{da}{a^3} db \frac{d\theta}{4\pi} \tag{8}$$

The Radon transform for an object f is the collection of line integrals indexed by $(\theta, t) \in [0, 2\pi) \times \mathbf{R}$ and is given by:

$$Rf(\theta, t) = \int_{-\infty}^{\infty} \int_{-\infty}^{\infty} f(x_1, x_2) \times \delta(x_1 \cos \theta + x_2 \sin \theta - t) dx_1 dx_2 \tag{9}$$

Thus, the ridgelet transform can be represented in terms of the Radon transform as follow:

$$R_f(a, b, \theta) = \int\limits_{-\infty}^{\infty} Rf(\theta, t) a^{-1/2} \left(\frac{(t-b)}{a} \right) dt \qquad (10)$$

Hence, the ridgelet transform is the application of the 1-D wavelet transform to the slices of the Radon transform where the angular variable θ is constant and t is varying. A schematic diagram of the ridgelet transform is shown in Fig. 3. To make the ridgelet transform discrete, both the Radon transform and the wavelet transform have to be discrete [9, 10].
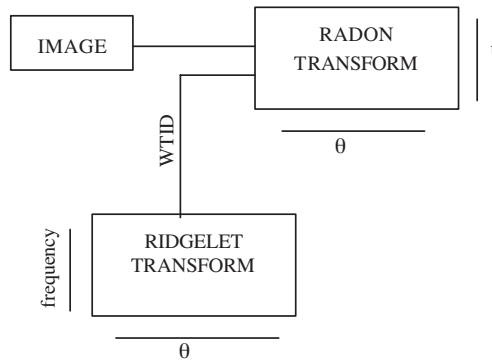
Figure 3. Ridgelet transform of an image.

4. THE PROPOSED FUSION ALGORITHM

It is known that different imaging modalities are employed to depict different anatomical morphologies. CT images are mainly employed to visualize dense structures such as bones. So, they give the general shapes of objects and few details. On the other hand, MR images are used to depict the morphology of soft tissues. So, they are rich in details [12–16]. Since these two modalities are of a complementary nature, our objective is to merge both images to obtain as much information as possible.

A curvelet based algorithm is introduced for this purpose. This algorithm is summarized as follows:

(1) The MR and the CT images are registered.
(2) The curvelet transform steps are performed on both images.

(3) The maximum frequency fusion rule is used for the fusion of the ridgelet transforms of the subbands Δ_1 and Δ_2 of both images.

(4) An inverse curvelet transform step is performed on P_3 of the MR image and the fused subbands Δ_1 and Δ_2.

These steps are expected to merge the details in both images into a single image with much more details.

5. EXPERIMENTAL RESULTS

The proposed algorithm for the fusion of MR and CT images is tested and compared to the traditional wavelet fusion algorithm. Two experiments are conducted for this purpose. For the evaluation of the performance of the fusion algorithms, the visual quality of the obtained fusion result as well as the quantitative analysis are used. The root mean square error of the fusion result is given by :

$$RMSE = \sqrt{\frac{\sum_{i=1}^{M}\sum_{j=1}^{N}[R(i,j) - F(i,j)]^2}{M \times N}} \qquad (11)$$

where $R(i,j)$ is either the MR or the CT image and $F(i,j)$ is the fusion result. M and N are the dimensions of the images to be fused. The smaller the value of the RMSE, the better the performance of the fusion algorithm. The PSNR of the fusion result is defined as follows:

$$PSNR = 10 \times \log\left((f_{\max})^2 / RMSE^2\right) \qquad (12)$$

where $f_{\max}$ is the maximum gray scale value of the pixels in the fused image. The higher the value of the PSNR, the better the performance of the fusion algorithm. The RMSE between the fusion result and both the MR and the CT images is estimated and two values of PSNR for both the curvelet and the wavelet fusion results are obtained. In the first experiment, CT and MR scans of the brain are used as shown in Figs. 4 and 5, respectively. The wavelet fusion result is given in Fig. 6 and the curvelet fusion result is given in Fig. 7. From the fusion results of Figs. 6 and 7, it is clear that the curvelet fusion result has a better visual quality than the wavelet fusion result. The PSNR values of these results are tabulated in Table 1. Another experiment has also been carried out on two other CT and MR images of the same object and the results are tabulated in Table 2. These values reflect the ability of the curvelet transform to capture features from both the MR and the CT images. From these results, it is clear that the proposed curvelet
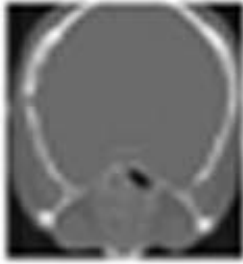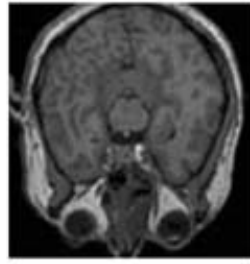
Figure 4. CT image.
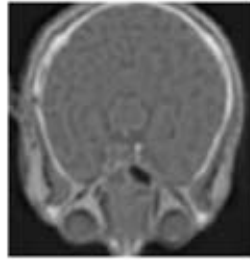

Figure 5. MR image.

Figure 6. Wavelet fusion.

Figure 7. Curvelet fusion.

Table 1. PSNR fusion results of experiment 1.

Method	PSNR
Wavelet	$PSNR_1$ =14.3 dB Fused image with MR image $PSNR_2$ = 22.8 dB Fused image with CT image
Curvelet	$PSNR_1$ = 15.2 dB Fused image with MR image $PSNR_2$ = 24.9 dB Fused image with CT image

Table 2. PSNR fusion results of experiment 2.

Method	PSNR
Wavelet	$PSNR_1$ =12.1 dB Fused image with MR image $PSNR_2$ = 14.6 dB Fused image with CT image
Curvelet	$PSNR_1$ = 12.5 dB Fused image with MR image $PSNR_2$ = 16.5 dB Fused image with CT image

fusion algorithm has succeeded in obtaining better results than the wavelet fusion algorithm from both the visual quality and the PSNR points of view.

6. CONCLUSION

The paper has presented a new trend in the fusion of MR and CT images which is based on the curvelet transform. A comparison study has been made between the traditional wavelet fusion algorithm and the proposed curvelet fusion algorithm. The experimental study shows that the application of the curvelet transform in the fusion of MR and CT images is superior to the application of the traditional wavelet transform. The obtained curvelet fusion results have higher PSNR values than the wavelet fusion results. Also, curved visual details are better in the curvelet fusion results than in the wavelet fusion results.

REFERENCES

1. Choi, M., R. Y. Kim, and M. G. Kim, "The curvelet transform for image fusion," *International Society for Photogrammetry and Remote Sensing, ISPRS 2004*, Vol. 35, Part B8, 59–64, Istanbul, 2004.
2. Choi, M., R. Y. Kim, M. R. Nam, and H. O. Kim, "Fusion of multispectral and panchromatic satellite images using the curvelet transform," *IEEE Geosci. Remote Sensing Lett.*, Vol. 2, No. 2, 136–140, Apr. 2005.
3. Niuñez, J., X. Otazu, O. Fors, A. Prades, V. Pala, and R. Arbiol, "Multiresolution-based image fusion with additive wavelet decomposition," *IEEE Trans. Geosci. Remote Sensing*, Vol. 37, No. 3, 1204–1211, May 1999.
4. Udomhunsakul, S. and P. Wongsita, "Feature extraction in medical MRI images," *Proceeding of 2004 IEEE Conference on Cybernetics and Intelligent Systems*, Vol. 1, 340–344, Dec. 2004.
5. Wang, A., H. J. Sun, and Y. Y. Guan, "The application of wavelet transform to multi-modality medical image fusion," *Proceedings of the 2006 IEEE International Conference on Networking, Sensing and Control, (ICNSC)*, 270–274, 2006.
6. Garzelli, A., F. Nencini, L. Alparone, and S. Baronti, "Multiresolution fusion of multispectral and panchromatic images through the curvelet transform," *Proceedings of IEEE International Geoscience and Remote Sensing Symposium, (IGARSS)*, Vol. 4, 2838–2841, 2005.
7. Shen, Y., J. C. Ma, and L. Y. Ma, "An adaptive pixel-weighted image fusion algorithm based on local priority for CT and MRI images," *Proceedings of the IEEE Instrumentation and Measurement Technology Conference, (IMTC)*, 420–422, 2006.

8. Saevarsson, B. B., J. R. Sveinsson, and J. A. Benediktsson, "Combined wavelet and curvelet denoising of SAR images," *Proceedings of IEEE International Geoscience and Remote Sensing Symposium, (IGARSS)*, Vol. 6, 4235–4238, 2004.

9. Saevarsson, B. B., J. R. Sveinsson, and J. A. Benediktsson, "Translation invariant combined denoising algorithm," *IEEE International Symposium on Circuits and Systems, (ISCAS 2005)*, Vol. 5, 4241–4244, 2005.

10. Saevarsson, B. B., J. R. Sveinsson, and J. A. Benediktsson, "Time invariant curvelet denoising," *Proceeding of the Nordic Signal Processing Symposium, (NORSIG 2004)*, 117–120, 2004.

11. Abd-El-samie, F. E., "Superresolution reconstruction of image," Ph.D. thesis, University of Menoufia, Egypt, 2005.

12. Yamamura, Y., K. Hyoungseop, and Y. Akiyoshi, "A method for image registration by maximization of mutual information," *SICE-ICASE International Joint Conference*, 1469–1472, 2006.

13. ÇALI‗IR, C., C. Korkmaz, and T. Kaya, "Comparison of MRI and CT in the diagnosis of early sacroiliitis," *The Medical Journal of Kocatepe*, 49–56, 2006.

14. Munir, S., "MRI scanner," *Proceedings of the First Regional Conference IEEE of the Biomedical Engineering Society of India*, 3/69–3/70, Feb. 1995.

15. Gilbert, B., "The multimodality imaging challenge in radiotherapy (RT)," Radiotherapy Department of Pitié-Salpétrière Hospital Paris, France.

16. Tomazevic, D., B. Likar, T. Slivnik, and F. Pernus, " 3-D/2-D registration of CT and MR to X-ray images," *IEEE Transactions on Medical Imaging*, Vol. 22, 1407–1416, 2003.

17. Li, S., J. T.-Y. Kwok, I. W.-H. Tsang, and Y. Wang, "Fusing images with different focuses using support vector machines," *IEEE Trans. Neural Networks*, Vol. 15, No. 6, 1555–1561, Nov. 2004.